Gap Structure of the Hofstadter System of Interacting Dirac Fermions in Graphene

Vadim M. Apalkov
Department of Physics and Astronomy, Georgia State University, Atlanta, Georgia 30303, USA

Tapash Chakraborty*
Department of Physics and Astronomy, University of Manitoba, Winnipeg, Canada R3T 2N2

(Received 13 November 2013; published 30 April 2014)

The effects of mutual Coulomb interactions between Dirac fermions in monolayer graphene on the Hofstadter energy spectrum are investigated. For two flux quanta per unit cell of the periodic potential, interactions open a gap in each Landau level with the smallest gap in the $n = 1$ Landau level. For more flux quanta through the unit cell, where the noninteracting energy spectra have many gaps in each Landau level, interactions enhance the low-energy gaps and strongly suppress the high-energy gaps and almost close a high-energy gap for $n = 1$. The signature of the interaction effects in the Hofstadter system can be probed through magnetization, which is governed by the mixing of the Landau levels and is enhanced by the Coulomb interaction.

DOI: 10.1103/PhysRevLett.112.176401 PACS numbers: 71.10.Pm, 73.20.At, 73.21.Cd

The dynamics of an electron in a periodic potential subjected to a perpendicular magnetic field has a long history [1–4]. Hofstadter's numerical solution of the Harper equation [2] in the tight-binding model demonstrated in 1976 that [4] the magnetic field splits the Bloch bands into subbands and gaps. The resulting energy spectrum, when plotted as a function of the magnetic flux per lattice cell reveals a fractal pattern that is known in the literature as Hofstadter's butterfly (due to the pattern resembling butterflies). A few experimental efforts to detect the butterflies have been reported in the literature. The earlier ones involved artificial lateral superlattices on semiconductor nanostructures [5–7], more precisely antidot lattice structures with periods of ~100 nm. The large period (as opposed to those in natural crystals) of the artificial superlattices helps to keep the magnetic field in a reasonable range of values to observe the fractal pattern. Measurements of the quantized Hall conductance in such a structure indicated, albeit indirectly, the complex pattern of gaps that was expected in the butterfly spectrum. Hofstadter butterfly patterns were also predicted to occur in other totally unrelated systems, such as, propagation of microwaves through a waveguide with a periodic array of scatterers [8] or more recently, with ultracold atoms in optical lattices [9].

Dirac fermions in monolayer and bilayer graphene [10–12] have been found to be the most promising objects thus far, where the signature of the recursive pattern of the Hofstadter butterfly has been unambiguously reported [13–15]. Here the periodic lattice with a period of ~10 nm was created by the moiré pattern that appears when graphene is placed on hexagonal boron nitride with a twist [16,17]. Although the period here is much shorter than that in semiconductor nanostructures, the unique properties of graphene help to create a robust butterfly pattern [18]. Theoretical studies of the butterfly pattern in monolayer [19] and bilayer graphene [20] systems were also reported earlier.

In comparison to the numerous studies of noninteracting fermions in the butterfly problem, there are very few papers that report on the effects of electron-electron interactions on the fractal energy spectra. Hartree [21] or mean-field approaches, reported earlier in conventional two-dimensional electron systems [22,23], indicated that although the butterfly pattern remains intact, additional gap structures are generated by the Coulomb interaction. The unique magnetic properties of Dirac fermions in graphene [11,12,24], however, provide a new frontier for exploration of the intricate structure of the magnetic butterflies. As stated above, graphene seems to be the best system in which to observe the fractal energy spectrum. Therefore, it is important to understand the role interacting Dirac fermions play in the Hofstadter spectrum in graphene. Here, we present our studies of the gap structure in the energy spectra due to the Coulomb interaction between Dirac fermions in monolayer graphene. Coulomb interaction in the presence of a strong magnetic field plays an important role in monolayer and bilayer graphene [10–12,24–26]. However, it is quite a challenging task to evaluate the role of Coulomb interactions in the present system due to the complexities of the Hofstadter energy spectra. Our studies indicate that the influence of the Coulomb interaction on the energy gap is highly nontrivial in this case. This is also reflected in the magnetization in the Hofstadter model of graphene.

We consider a monolayer graphene in a periodic external potential that has the following form

$$V(x, y) = V_0[\cos(q_x x) + \cos(q_y y)], \quad (1)$$

where V_0 is the amplitude of the periodic potential, $q_x = q_y = q_0 = 2\pi/a_0$, and a_0 is a period of the external potential $V(x, y)$. We begin with the single-particle energy spectrum of the electron system in the periodic potential (1) and in an external perpendicular magnetic field B. The corresponding Hamiltonian then is

$$\mathcal{H} = \mathcal{H}_B + V(x, y), \tag{2}$$

where $\mathcal{H}_B$ is the Hamiltonian of an electron in graphene in a perpendicular magnetic field. The electron energy spectrum of graphene in a magnetic field has twofold spin and twofold valley degeneracy. This degeneracy cannot be lifted by the periodic potential. In that case, for the single-electron system we consider the spectrum for a given valley, say valley K, and a given component of the spin. The corresponding Hamiltonian $\mathcal{H}_B$ can now be written [11,12,24]

$$\mathcal{H}_B = \frac{\gamma}{\hbar}\begin{pmatrix} 0 & \pi_x - i\pi_y \\ \pi_x + i\pi_y & 0 \end{pmatrix}, \tag{3}$$

where $\vec{\pi} = \vec{p} + e\vec{A}/c$, $\vec{p}$ is the electron momentum (two dimensional), $\vec{A} = (0, Bx, 0)$ is the vector potential, and γ is the band parameter.

We evaluate the energy spectrum of an electron in a magnetic field and a periodic potential expressing the Hamiltonian (2) in the basis of eigenfunctions of the Hamiltonian (3). These eigenfunctions are specified by the Landau index $n = 0, \pm 1, \pm 2, \cdots$ and a parameter k, which is the y component of the wave vector. The eigenfunctions of the Hamiltonian (3) are given by

$$\Psi_{n,k} = C_n \begin{pmatrix} \mathrm{sgn}(n) i^{|n|-1} \varphi_{|n|-1,k} \\ i^{|n|} \varphi_{|n|,k} \end{pmatrix}, \tag{4}$$

where $C_n = 1$ for $n = 0$ and $C_n = 1/\sqrt{2}$ for $n \neq 0$, $\mathrm{sgn}(n) = 1$ for $n > 0$, $\mathrm{sgn}(n) = 0$ for $n = 0$, and $\mathrm{sgn}(n) = -1$ for $n < 0$. Here $\varphi_{n,k}$ is the electron wave function with a parabolic dispersion relation in the nth Landau level (LL)

$$\varphi_{n,k}(x, y) = \frac{e^{iky}}{\sqrt{L}} \frac{e^{-(x-x_k)^2/2\ell_0^2}}{\sqrt{\pi^{1/2}\ell_0 2^n n!}} H_n(x - x_k), \tag{5}$$

where L is the length in the y direction, $x_k = k\ell_0^2$, $\ell_0 = \sqrt{c\hbar/eB}$ is the magnetic length, and $H_n(x)$ are the Hermite polynomials. The eigenenergy corresponding to the wave function (4) is $\varepsilon_n = \mathrm{sgn}(n)\hbar\omega_B\sqrt{|n|}$ [11,12,24].

We evaluate the matrix elements of the periodic potential $V(x, y)$ in the basis $\Psi_{n,k}(x, y)$ and construct the single-particle Hamiltonian matrix in the basis of the wave functions (4). In what follows, we consider only the basis states for $n = 0$, $n = \pm 1$, and $n = \pm 2$ LLs of graphene. Inclusion of higher LL states does not change considerably the results for the band gaps presented below. From the Hamiltonian matrix we evaluate the energy spectrum of Dirac fermions in a magnetic field and a periodic potential. The corresponding spectra are shown in Fig. 1 for $n = 0$ and $n = \pm 1$ Landau levels. The energy spectra are shown as a function of the magnetic field in terms of the parameter $\alpha = \phi_0/\phi$, where $\phi = Ba_0^2$ is the magnetic flux through the unit cell of the periodic potential and $\phi_0 = h/e$ is the flux quantum. The energy spectra clearly show the fractal butterfly structure. For small values of V_0 the coupling of the states of different LLs is small, and in each LL, for $\alpha = p/q$ with integer p and q, there are q bands. With increasing V_0 the coupling of the states of different LLs becomes strong, which results in a strong overlap of different Landau bands.

With the single-particle states at our disposal, we now calculate the matrix elements of the electron-electron (Coulomb) interaction and find the single-particle energy spectrum of the corresponding Hartree Hamiltonian. Since the electron density has the same periodic behavior as the periodic potential, the Fourier components of the Hartree potential are nonzero only for the discrete reciprocal vectors $\vec{G}$ and can be found from $V(\vec{G}) = (2\pi e^2/\kappa|\vec{G}|)n(\vec{G})$ and $V(0) = 0$. Here $n(\vec{G})$ is the Fourier component of the electron density that is determined by the occupied levels. For the many-particle system, we consider only $n = 0$, $n = \pm 1$, and $n = \pm 2$. We also restrict the number of states in a given LL; i.e., we consider a finite size system with 5000 states per LL with the interwave vector separation $\Delta k = q_0/50$, where the one-dimensional wave vector k determines the electron state [see Eq. (5)]. This corresponds to the size of the system in the real space being $50a_0 \times 50a_0$. To eliminate the boundary effects we consider the periodic boundary conditions. Due to the finite size of the system it is difficult to identify and trace the band structure of the energy spectra for generic rational

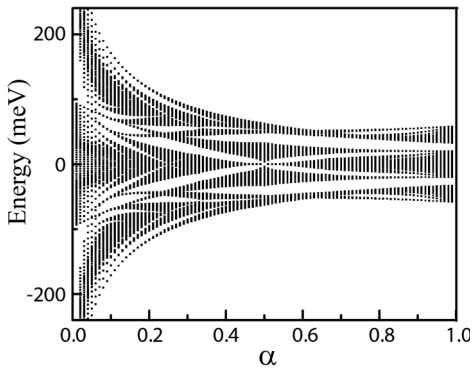

FIG. 1. Single-electron energy spectra of Dirac fermions in graphene in a magnetic field and a periodic potential $V(x, y)$ with period $a_0 = 20$ nm and amplitude $V_0 = 35$ meV. The energy spectra are shown as a function of the number of flux quanta per unit cell. The results are for the $n = 0$ and $n = \pm 1$ LLs.

values p/q of α. Therefore, in what follows, the interaction effects on the band structure of graphene were studied for $\alpha = 1/2$ and $\alpha = 1/3$. For a noninteracting system at $\alpha = 1/2$, in each LL there are two bands with zero band gap. In this case the interelectron interaction opens a finite gap. For $\alpha = 1/3$, both noninteracting and interacting electron systems have three bands with two finite band gaps in each LL.

The effects of interaction on the band structure also depend on the LL filling. We present the main results for half filling of the $n = 0$ LL, which is defined through zero Fermi energy. The single-particle spectra show the band structure with two bands in each LL. An increase in amplitude of the periodic potential causes both the band gap and band widths to increase in each LL.

The influence of electron-electron interactions on the band gaps Δ_n for $\alpha = 1/2$ is plotted in Fig. 2 as a function of V_0. Here the band gap for the LL n is labeled as Δ_n. Noninteracting systems have zero gaps and are not shown here. The results are for $a_0 = 20$ [Fig. 2(a)] and 40 nm [Fig. 2(b)]. In general, in both cases the band gaps monotonically increase with V_0. With the Landau level index the band gaps have a strong nonmonotonic dependence, where the band gap for $n = 1$ is much smaller than those for $n = 0$ and $n = 2$ [27]. For the $n = 1$ gap there is also a small nonmonotonic dependence of Δ_1 on V_0 with a local maximum for $V_0 \approx 17$ meV.

The $\alpha = 1/3$ results are shown in Fig. 3. In this case, both the noninteracting and interacting systems have three bands in each LL with two corresponding gaps. We label these gaps as $\Delta_{n,i}^{(0)}$ (noninteracting) and $\Delta_{n,i}$ (interacting). Here $i = 1, 2$ is the number of the band gap: $i = 1$—low-energy gap and $i = 2$—high-energy gap. In the lowest LL [Figs. 3(a) and 3(d)], which is partially occupied, the gaps monotonically increase with V_0. The interaction enhances the low-energy gap Δ_{01} and suppresses the higher energy gap Δ_{02}. This suppression decreases with increasing period of the potential, a_0. Similar behavior is also observed for $n = 1$ [Figs. 3(b) and 3(c)], but now the suppression of the higher energy gap is large compared to the $n = 0$ case. The gap Δ_{12} becomes vanishingly small for low periods of the potential. Therefore, the interelectron interactions almost close one of the gaps in the energy dispersion for $n = 1$. For $n = 2$ the main effect of the interaction is a strong enhancement of the low-energy gap Δ_{21}, while the higher energy gap is almost unaffected by the interaction.

The general effects of the electron-electron interaction on the band structure of the energy dispersion is therefore an enhancement of the low-energy gaps and suppression of the higher energy gaps (within a single LL). This suppression can be attributed to the interstate repulsion introduced by the interaction between the states of the $n = 0$ LL and the states of higher LLs. The repulsion becomes weaker when the energy separation between the states increases. For $n = 1$, which is the closest to the $n = 0$ LL the effect of state repulsion is more pronounced, which results in almost collapsing of the high-energy gap. The energy gaps (and the corresponding energy spectra) versus V_0 approximately depend on $V_0/\hbar\omega_B \propto V_0 a_0$ [or $V_0/(e^2/\ell_0) \propto V_0 a_0$]. The minimum of Δ_{22} in Fig. 3(f), for example, is therefore also visible in Fig. 3(c), but at higher values of V_0.

The above results (Figs. 2 and 3) are for the half-filled $n = 0$ LL, which corresponds to zero Fermi energy. Variation of the population in the $n = 0$ LL, which can be described numerically in terms of variation of the Fermi energy, also changes the gaps. As an illustration of this

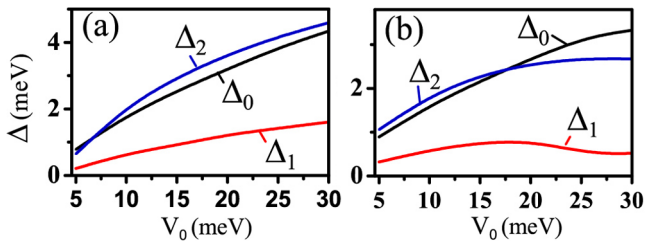

FIG. 2 (color online). The band gaps in the $n = 0$, $n = 1$, and $n = 2$ LLs versus the amplitude of the periodic potential, V_0, for interacting systems with half filling of the $n = 0$ LL. The band gaps are defined as the gaps between the corresponding bands of Dirac fermions in a magnetic field corresponding to $\alpha = 1/2$. The period of the potential is (a) $a_0 = 20$ nm and (b) $a_0 = 40$ nm.

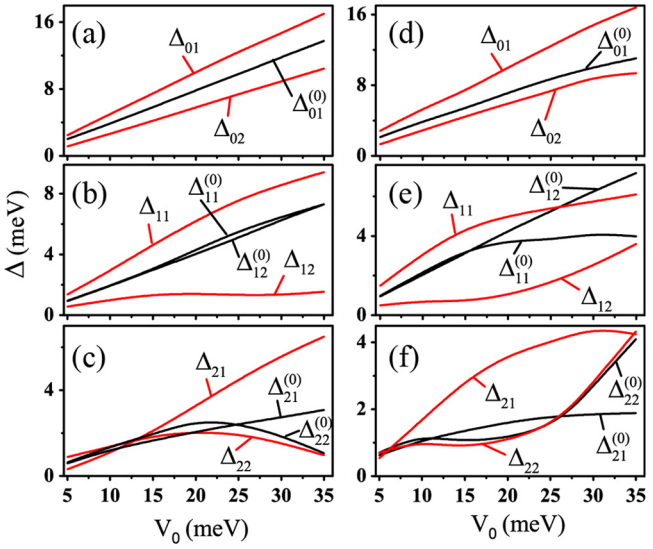

FIG. 3 (color online). The band gaps versus V_0 for $n = 0$ (a), (d), $n = 1$ (b),(e), and $n = 2$ (c),(f) LLs. The band gaps are defined as the gaps between the corresponding bands of Dirac fermions in a magnetic field for $\alpha = 1/3$. The black lines correspond to the case of the noninteracting system, while the red or medium gray lines correspond to the Dirac fermions with Hartree interaction and half filling of the $n = 0$ LL. The gaps are labeled as $\Delta_{ni}^{(0)}$ (noninteracting system) and Δ_{ni} (interacting system), where n is the LL index and $i = 1$ and 2 correspond to the low-energy and high-energy gaps, respectively. The period of the periodic potential is 20 nm (a)–(c) and 40 nm (d)–(f).

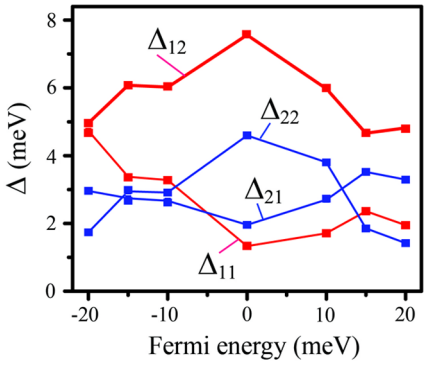

FIG. 4 (color online). The band gaps for $n = 1$ and $n = 2$ LLs as a function of the Fermi energy for electrons in $n = 0$, i.e., as a function of the population of the $n = 0$ LL and for a magnetic field corresponding to $\alpha = 1/3$. The period and amplitude of the potential are $a_0 = 20$ nm and $V_0 = 25$ meV, respectively. The zero Fermi energy corresponds to half filling of the $n = 0$ LL.

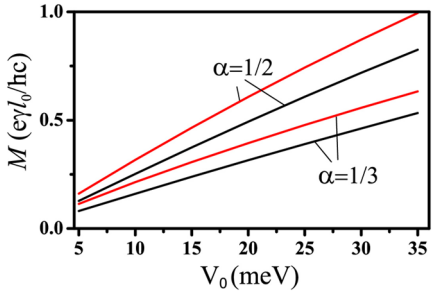

FIG. 5 (color online). Magnetization of Dirac fermions as a function of the amplitude of V_0 for noninteracting (black line) and interacting (red or medium gray line) systems and for two values of the parameter α. The filling factor of the $n = 0$ LL is $\nu = 1/2$.

dependence, in Fig. 4 the gaps $\Delta_{1,i}$ and $\Delta_{2,i}$ are shown as a function of the Fermi energy. This dependence reveals that the difference between the gaps in the same LL (i.e., between Δ_{11} and Δ_{12}) is the largest for zero Fermi energy. Therefore, in this case we should expect the strongest interaction effect on the energy spectra and the corresponding gaps.

Both the periodic potential and the electron-electron interaction cause mixing of the states of different LLs. The typical energy scale of the Coulomb interaction corresponding to the periodic potential with period a_0 is $e^2/\kappa a_0 \approx 20$ meV for $a_0 = 20$ nm and the dielectric constant $\kappa = 4$. For the inter-Landau separation ≈50 meV, this interaction strength results in a LL mixing. The periodic potential, which can be of the same order as the interaction strength, also introduces LL mixing, which increases with increasing V_0. Since the magnetic field is proportional to $1/\alpha$ with decreasing α the inter-Landau level energy separation increases, which should suppress the interlevel mixing due to the interelectron interactions and the periodic potential.

A measurable quantity of the many-fermion system that depends on the LL mixing and can exhibit the effect of the electron-electron interaction is the magnetization $M = (\partial\mathcal{H}/\partial B)$ [28], where the dependence of the Hamiltonian on the magnetic field is introduced through the vector potential $\vec{A}$. For the many-fermion system the magnetization operator is the sum of the single-particle contributions. The magnetization is then calculated as an expectation value of the magnetization operator.

The magnetization of the noninteracting system and the system with electron-electron interactions is shown in Fig. 5. For the noninteracting system the magnetization increases monotonically with increasing strength of V_0. The reason for such an increase is the enhancement of the LL mixing with increasing V_0. Without the LL mixing, the Dirac fermions in the $n = 0$ LL have zero magnetization for all magnetic fields B, which follows from the fact that the energy of the $n = 0$ LL is zero for all B [11,12,24]. Therefore, the nonzero magnetization illustrates the strength of the LL mixing. For the interacting system the magnetization monotonically increases with V_0 and shows enhancement compared to the noninteracting system. With increasing V_0 the mixing of the levels due to interaction increases both for $\alpha = 1/2$ and $\alpha = 1/3$. The magnetization increases with increasing α, which illustrates a stronger interlevel mixing for larger values of α.

In conclusion, the interaction effects on the Hofstadter system in monolayer graphene strongly depend on the amplitude of the periodic potential. For $\alpha = 1/2$, the interaction opens a gap in each LL, with the gap being smaller for $n = 1$. For larger numbers of flux quanta per unit cell, such as $\alpha = 1/3$, the interaction suppresses the high-energy gaps and enhances the low-energy gaps compared to the noninteracting system. The effect is strongest for $n = 1$ where the high-energy gap is almost closed by the interaction. The magnetization of the system illustrates the enhancement of level mixing due to the interaction. This enhancement increases with increasing V_0 and the level mixing becomes stronger with increasing α.

The work has been supported by the Canada Research Chairs Program of the Government of Canada.

*Tapash.Chakraborty@umanitoba.ca

[1] U. Rössler and M. Shurke, in *Advances in Solid State Physics*, edited by B. Kramer (Springer, Berlin, 2000), Vol. 40, pp. 35–50.
[2] P. G. Harper, Proc. Phys. Soc. London **68**, 874 (1955).
[3] D. Langbein, Phys. Rev. **180**, 633 (1969).
[4] D. Hofstadter, Phys. Rev. B **14**, 2239 (1976).
[5] M. C. Geisler, J. H. Smet, V. Umansky, K. von Klitzing, B. Naundorf, R. Ketzmerick, and H. Schweizer, Phys. Rev. Lett. **92**, 256801 (2004); Physica (Amsterdam) **25E**, 227 (2004).

[6] C. Albrecht, J. H. Smet, K. von Klitzing, D. Weiss, V. Umansky, and H. Schweizer, Phys. Rev. Lett. **86**, 147 (2001); Physica (Amsterdam) **20E**, 143 (2003).
[7] T. Schlösser, K. Ensslin, J. P. Kotthaus, and M. Holland, Europhys. Lett. **33**, 683 (1996); Semicond. Sci. Technol. **11**, 1582 (1996).
[8] U. Kuhl and H.-J. Stöckmann, Phys. Rev. Lett. **80**, 3232 (1998).
[9] M. Aidelsburger, M. Atala, M. Lohse, J. T. Barreiro, B. Paredes, and I. Bloch, Phys. Rev. Lett. **111**, 185301 (2013); H. Miyake, G. A. Siviloglou, C. J. Kennedy, W. C. Burton, and W. Ketterle, Phys. Rev. Lett. **111**, 185302 (2013).
[10] D. S. L. Abergel and T. Chakraborty, Phys. Rev. Lett. **102**, 056807 (2009).
[11] *Physics of Graphene*, edited by H. Aoki and M. S. Dresselhaus (Springer, New York, 2014).
[12] D. S. L. Abergel, V. Apalkov, J. Berashevich, K. Ziegler, and T. Chakraborty, Adv. Phys. **59**, 261 (2010).
[13] C. R. Dean, L. Wang, P. Maher, C. Forsythe, F. Ghahari, Y. Gao, J. Katoch, M. Ishigami, P. Moon, M. Koshino, T. Taniguchi, K. Watanabe, K. L. Shepard, J. Hone, and P. Kim, Nature (London) **497**, 598 (2013).
[14] B. Hunt, J. D. Sanchez-Yamagishi, A. F. Young, M. Yankowitz, B. J. LeRoy, K. Watanabe, T. Taniguchi, P. Moon, M. Koshino, P. Jarillo-Herrero, and R. C. Ashoori, Science **340**, 1427 (2013).
[15] L. A. Ponomarenko, R. V. Gorbachev, G. L. Yu, D. C. Elias, R. Jalil, A. A. Patel, A. Mishchenko, A. S. Mayorov, C. R. Woods, J. R. Wallbank, M. Mucha-Kruczynski, B. A. Piot, M. Potemski, I. V. Grigorieva, K. S. Novoselov, F. Guinea, V. I. Falko and A. K. Geim, Nature (London) **497**, 594 (2013).
[16] R. Decker, Y. Wang, V. W. Brar, W. Regan, H.-Z. Tsai, Q. Wu, W. Gannett, A. Zettl, and M. F. Crommie, Nano Lett. **11**, 2291 (2011).
[17] J. Xue, J. Sanchez-Yamagishi, D. Bulmash, P. Jacquod, A. Deshpande, K. Watanabe, T. Taniguchi, P. Jarillo-Herrero, and B. J. LeRoy, Nat. Mater. **10**, 282 (2011).
[18] A superlattice with a shorter period requires a larger magnetic field to fill up the unit cell. The larger magnetic field values make for larger Landau level separation in general. In graphene, the Landau level separation is larger for low filling fractions than in conventional semiconductor systems due to the linear dispersion relation. Further, the superlattice modulation potential between graphene and the hexagonal boron nitride is ∼10 meV, which is quite substantial. All of these attributes make the butterfly spectrum more robust in graphene; P. Kim (private communication).
[19] J.-W. Rhim and K. Park, Phys. Rev. B **86**, 235411 (2012).
[20] N. Nemec and G. Cuniberti, Phys. Rev. B **75**, 201404 (2007); R. Bistritzer and A. H. MacDonald, Phys. Rev. B **84**, 035440 (2011).
[21] V. Gudmundsson and R. R. Gerhardts, Surf. Sci. **361**, 505 (1996); Phys. Rev. B **52**, 16744 (1995); Phys. Rev. B **54**, R5223 (1996).
[22] A. Kol and N. Read, Phys. Rev. B **48**, 8890 (1993).
[23] H. Doh and S.-H. Suck Salk, Phys. Rev. B **57**, 1312 (1998).
[24] T. Chakraborty and V. M. Apalkov, Solid State Commun. **175**, 123 (2013).
[25] V. M. Apalkov and T. Chakraborty, Phys. Rev. Lett. **97**, 126801 (2006).
[26] V. M. Apalkov and T. Chakraborty, Phys. Rev. Lett. **105**, 036801 (2010);V. M. Apalkov and T. Chakraborty, Phys. Rev. Lett. **107**, 186803 (2011).
[27] The reason for $\Delta_1 < \Delta_2$ between the gaps is that the Coulomb interaction strength between the electrons in the $n = 0$ and $n = 1$ LLs is less by $\approx$3.5 meV than that between the electrons in the $n = 0$ and $n = 2$ LLs. The interaction potential was evaluated for the wave vector $\approx 2\pi/a_0$.
[28] See, for example, J. P. Eisenstein, H. L. Stormer, V. Narayanamurti, A. Y. Cho, A. C. Gossard, and C. W. Tu, Phys. Rev. Lett. **55**, 875 (1985); I. Meinel, D. Grundler, S. Gargstädt-Franke, C. Heyn, and D. Heitmann, Appl. Phys. Lett. **70**, 3305 (1997); I. Meinel, T. Hengstmann, D. Grundler, D. Heitmann, W. Wegscheider, and M. Bichler, Phys. Rev. Lett. **82**, 819 (1999); I. Meinel, D. Grundler, D. Heitmann, A. Manolescu, V. Gudmundsson, W. Wegscheider, and M. Bichler, Phys. Rev. B **64**, 121306 (2001); M. Zhu, A. Usher, A. J. Matthews, A. Potts, M. Elliott, W. G. Herrenden-Harker, D. A. Ritchie, and M. Y. Simmons, Phys. Rev. B **67**, 155329 (2003).